Empirical nucleus-nucleus potential deduced from fusion excitation functions

K. Siwek-Wilczyńska
Institute of Experimental Physics, Warsaw University, 00-681 Warsaw, Poland

J. Wilczyński
Institute for Nuclear Studies, 05-400 Otwock-Świerk, Poland

(Received 11 November 2003; published 26 February 2004)

Existing data on near-barrier fusion excitation functions for 48 medium and heavy nucleus-nucleus systems have been analyzed using a simple "diffused-barrier formula" derived assuming the Gaussian shape of the barrier height distributions. The obtained mean values of the barrier height have been used then for determination of the parameters of the empirical nucleus-nucleus potential, assumed to have Woods-Saxon shape. The mean barrier heights calculated with this potential are reproduced with an accuracy of about 1 MeV, while other frequently used potentials, i.e., the proximity potential and the Akyüz-Winther potential, considerably overpredict the experimental values, especially for heavy systems. In order to predict fusion excitation functions with the diffused-barrier formula, we propose a simple method of theoretical prediction of the second parameter of the barrier distribution, its width. The proposed formula accounts for the quantum effect of sub-barrier tunneling, static quadrupole deformations, and collective surface vibrations of the colliding nuclei. With the theoretical knowledge of the mean height and width of the barrier distributions, one can predict cross sections for overcoming the barrier ("sticking" or "capture") in reactions of very heavy systems used to produce superheavy nuclei.

DOI: 10.1103/PhysRevC.69.024611 PACS number(s): 25.70.Jj

I. INTRODUCTION

Nucleus-nucleus fusion reactions have been studied for many years with the aim to learn essential features of the fusion mechanism and to establish optimum conditions for synthesis of particular compound nuclei, for example, exotic nuclei far from β stability or new superheavy elements. In recent years special attention was paid to very precise measurements of fusion excitation functions at near- and sub-barrier energies. These precisely measured fusion excitation functions have been used to study the coupled-channel effects involving rotational, vibrational, and neutron-transfer channels influencing the fusion probabilities [1,2]. A numerous and very valuable set of precisely measured fusion excitation functions has been collected so far [2–19].

In the present work we analyze the collected set of fusion excitation functions within a simple model that allows us to determine the mean value of the fusion barrier and the width of the barrier distribution individually for each reaction. The deduced barrier heights are used then for determination of a semiempirical nucleus-nucleus potential in peripheral region of relative nucleus-nucleus distances.

II. FUSION BARRIER DISTRIBUTIONS

It is well known that fusion excitation functions cannot be satisfactorily explained assuming simply the penetration through a well-defined barrier in one-dimensional potential of a colliding nucleus-nucleus system. In order to reproduce shapes of experimentally observed fusion excitation functions, especially at low, near-threshold energies, it is necessary to assume a *distribution* of the fusion barrier height, the effect that results from the coupling to other than relative distance degrees of freedom. This is naturally achieved in coupled-channel calculations, involving the coupling to the lowest collective states in both colliding nuclei.

As demonstrated by Rowley, Satchler, and Stelson [1], the fusion barrier distribution can be deduced from a precisely measured fusion excitation function by taking the second derivative of the product of the cross section multiplied by energy,

$$P(E) = \frac{d^2(\sigma E)}{dE^2}. \tag{1}$$

Figure 1 shows examples of experimentally measured fusion excitation functions (top) and deduced [20] fusion barrier distributions (bottom) for two selected reactions: ^{40}Ca+^{96}Zr [12] and ^{34}S+^{168}Er [18]. The double differentiation of the dependence of σE on E requires very high precision of the measured cross sections. A typical approach used in most of published papers consists in using so-called "point difference formula" (see, e.g., a review paper by Dasgupta *et al.* [2]):

$$\frac{d^2(E\sigma)}{dE^2} = 2\left(\frac{(E\sigma)_3-(E\sigma)_2}{E_3-E_2} - \frac{(E\sigma)_2-(E\sigma)_1}{E_2-E_1}\right)\left(\frac{1}{E_3-E_1}\right), \tag{2}$$

where $(E\sigma)_i$ are calculated at three close energies E_i, and the value of $d^2(E\sigma)/dE^2$ is assigned to an energy $(E_1+2E_2+E_3)/4$. Results of this procedure depend very much on the energy distance between points 1 and 3. As the barrier distribution is naturally smeared out due to quantum tunneling by its finite width FWHM =2–3 MeV (see Sec. VI and Ref. [1]), the experimentally deduced barrier distribution

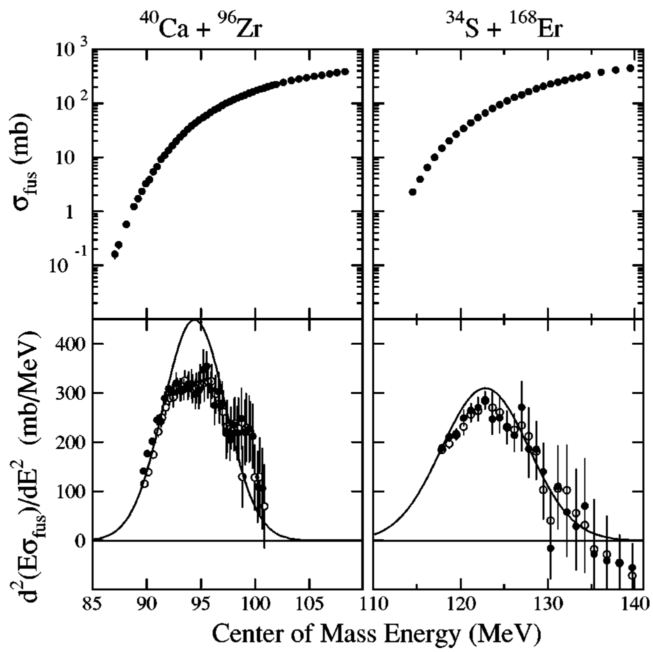

FIG. 1. Fusion excitation functions (top) and the deduced barrier distributions (bottom) for the ^{40}Ca+^{96}Zr [12] and ^{34}S+^{168}Er [18] reactions. The barrier distributions determined with the standard "point difference method" and the "polynomial fit method" are shown with full and open circles, respectively. The Gaussian-barrier distributions obtained by fitting the "diffused-barrier formula," Eq. (6), to the fusion excitation functions are shown by solid lines. After Ref. [20].

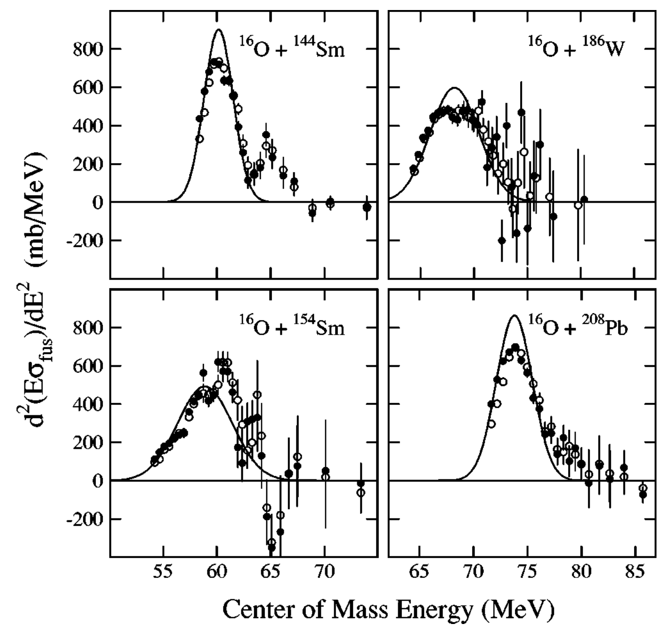

FIG. 2. The barrier distributions $d^2(E\sigma_{fus})/dE^2$ determined with the standard "point difference method" (full circles) and the "polynomial fit method" (open circles) for fusion reactions of ^{16}O ions with ^{144}Sm, ^{154}Sm, ^{184}W, and ^{208}Pb target nuclei. (Data taken from Refs. [10,14].) The Gaussian-barrier distributions obtained by fitting the "diffused-barrier formula," Eq. (6), are shown by solid lines. After Ref. [20].

should be smoothed over a similar range. Therefore the energy distance $\Delta E = E_3 - E_1 \approx 2(E_2 - E_1)$ is usually chosen to be 4–6 MeV.

In addition to experimental points evaluated with the point difference formula, Fig. 1 also shows equivalent points obtained in an alternative way [20], in which the experimental values of $E\sigma$ were locally fitted to the second-order polynomial,

$$E\sigma = a + bE + cE^2, \tag{3}$$

by using the least-square method. In this approach, a value of the coefficient c in the quadratic term determines $P(E) = d^2(E\sigma)/dE^2 = 2c$. It is seen from Fig. 1 that both methods yield comparable distributions, provided the energy span ΔE in both methods is the same.

In the present paper, we do not analyze and discuss specific structural effects that can be interpreted in terms of the coupled-channels calculations. (In addition to almost structureless distributions shown in Fig. 1, we present in Fig. 2 the fusion barrier distributions determined in four reactions [10,14] induced by ^{16}O ions on different target nuclei, showing a more distinct structure.) The observed structures in the barrier distributions result from tiny details in the measured excitation functions and their interpretation is often ambiguous. As mentioned above, the observed structure depends strongly on the choice of the energy span ΔE used in the analysis of the fusion excitation functions. Moreover, the error bars resulting from the numerical double differentiation of the $E\sigma$ values increase with energy, and practically eliminate possibility to observe any meaningful structure on the high-energy side of the barrier distribution.

In the following, we concentrate our analysis on the *overall* characteristics of the fusion barrier distributions, i.e., on determination of the mean value of the barrier and the width of its distribution. We are going to use the precise information on the mean barrier heights, collected for many nuclear systems, for determination of the parameters of the nucleus-nucleus potential. Then, knowing the empirical nucleus-nucleus potential deduced from experimentally determined fusion barriers, we will be able to predict the fusion or capture cross sections for not yet studied reactions.

III. FORMULA FOR OVERCOMING THE DIFFUSED BARRIER

In order to make a systematic overview of existing data on fusion excitation functions, we propose to use a simple formula for the cross section for *overcoming* the potential-energy barrier. In case of light and medium systems, the overcoming the barrier automatically leads to fusion of the colliding nuclei and formation of the compound nucleus. On the contrary, very heavy systems only stick together after overcoming the barrier and do not necessarily fuse, the effect known as the "hindrance factor." Therefore for those heavy systems the overcoming the barrier is identified with the "capture" cross section rather than fusion cross section.

Neglecting structure effects in the barrier distributions, we *assume* that these distributions have a Gaussian shape,

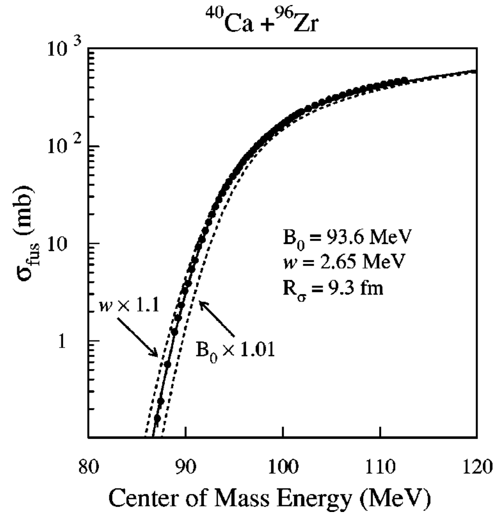

FIG. 3. Fusion excitation function for the ^{40}Ca + ^{96}Zr reaction, measured by Timmers *et al.* [12] (full circles), compared with the least-square fit of the "diffused-barrier formula," Eq. (6), shown by solid line. Dashed lines illustrate sensitivity of the calculated curve to the variation of the mean barrier B_0 increased by 1% and the width w increased by 10%.

$$p(B) = \frac{1}{w\sqrt{2\pi}} \exp\left[-\frac{(B-B_0)^2}{2w^2}\right], \tag{4}$$

with two parameters, the mean barrier B_0 and the distribution width w, to be determined individually for each reaction. By folding the barrier distribution, Eq. (4), with the classical expression for the fusion cross section

$$\sigma_{fus} = \pi R_\sigma^2\left(1 - \frac{B}{E}\right), \tag{5}$$

we obtain [21] the following formula for the energy dependence of the fusion cross section:

$$\sigma_{fus} = \pi R_\sigma^2 \frac{w}{E\sqrt{2\pi}}[X\sqrt{\pi}(1 + \operatorname{erf} X) + \exp(-X^2)], \tag{6}$$

where

$$X = \frac{E - B_0}{\sqrt{2}w}, \tag{7}$$

and erf X is the Gaussian error integral of the argument X. By R_σ we denote the relative distance corresponding approximately to the position of the barrier. Along with B_0 and w, R_σ is a parameter to be determined by fitting Eq. (6) to a given fusion excitation function.

In derivation of formula (6), the quantum effect of sub-barrier tunneling is not accounted for explicitly. However, the influence of the tunneling on shape of a given fusion excitation function is effectively included in the width parameter w. In Sec. VI we derive a simple formula for the width w, explicitly containing the sub-barrier tunneling component.

The "diffused-barrier formula," Eq. (6), is a very convenient parametrization of the cross section for a process of overcoming the potential-energy barrier. Therefore it can be successfully used for analysis and predictions of the fusion excitation functions of light, medium, and moderately heavy systems, especially in the range of near-barrier energies. For very heavy systems, when the overcoming the barrier does not guarantee fusion, predictions based on Eq. (6) give the capture or "sticking" cross section.

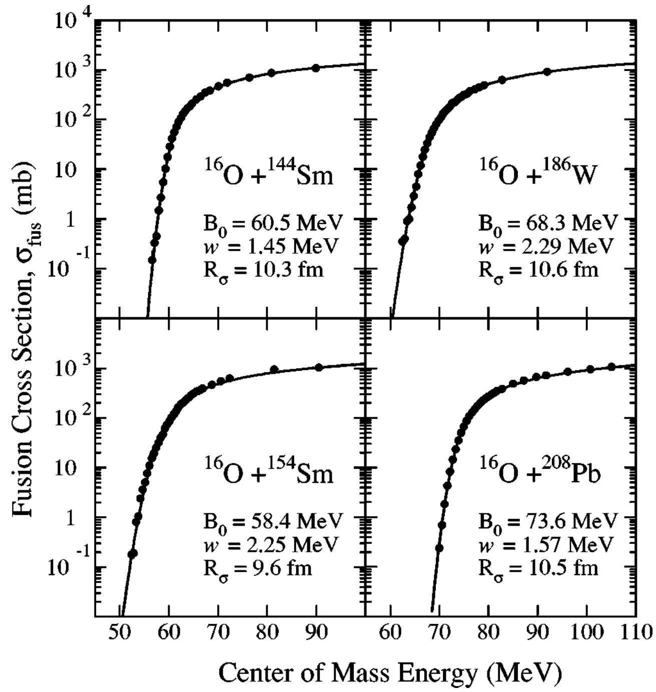

FIG. 4. Fusion excitation functions measured for the ^{16}O + ^{144,154}Sm [10], ^{16}O + ^{186}W, and ^{16}O + ^{208}Pb [14] reactions (full circles) compared with predictions (solid lines) of the "diffused-barrier formula," Eq. (6), for values of B_0, w, and R_σ obtained with the least-square method.

IV. ANALYSIS OF FUSION EXCITATION FUNCTIONS

In Fig. 3 we show one example of a fit of Eq. (6) to experimental data illustrating the quality of the fit and sensitivity of the calculated fusion excitation function to variation of the parameters. For this purpose we have chosen a very precisely measured fusion excitation function for the ^{40}Ca + ^{96}Zr reaction [12], the same that was used in Sec. II to demonstrate the method of empirical derivation of the barrier distribution. Formula (6) was fitted to the fusion excitation function using the least-square method, with variation of all three parameters: B_0, w, and R_σ. Different points in the excitation functions were equally weighted, i.e., the same relative error was assumed for all points, the assumption reflecting the fact that the systematic error of *absolute* determination of the fusion cross section plays the decisive role. It is seen that the fusion excitation function can be reproduced very accurately over the entire energy range, though the cross section varies by four orders of magnitude.

From Figs. 1 and 2, we can see that the Gaussian curves calculated with B_0 and w determined from fitting Eq. (6) (shown by solid lines) well agree with the barrier distribu-

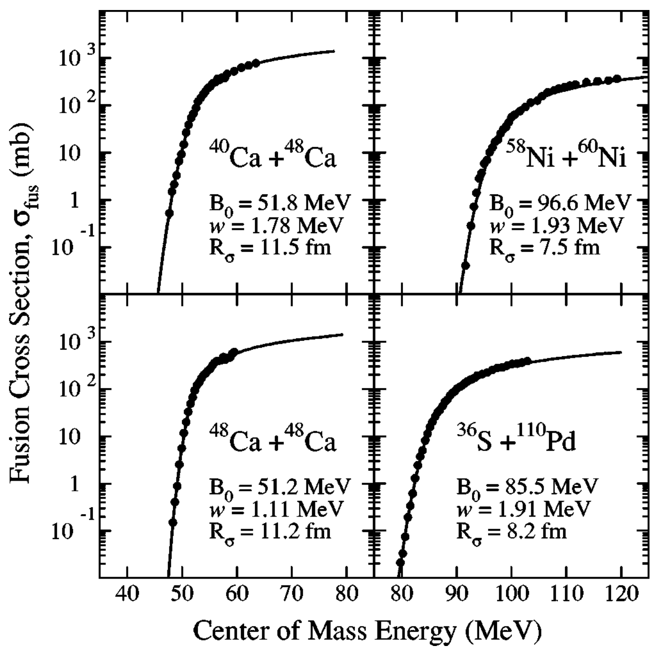

FIG. 5. Fusion excitation functions measured for the ^{48}Ca $+^{40,48}$Ca [19], ^{58}Ni$+^{60}$Ni [8], and ^{36}S$+^{110}$Pd [9] reactions (full circles) compared with predictions (solid lines) of the "diffused-barrier formula," Eq. (6), for values of B_0, w, and R_σ obtained with the least-square method.

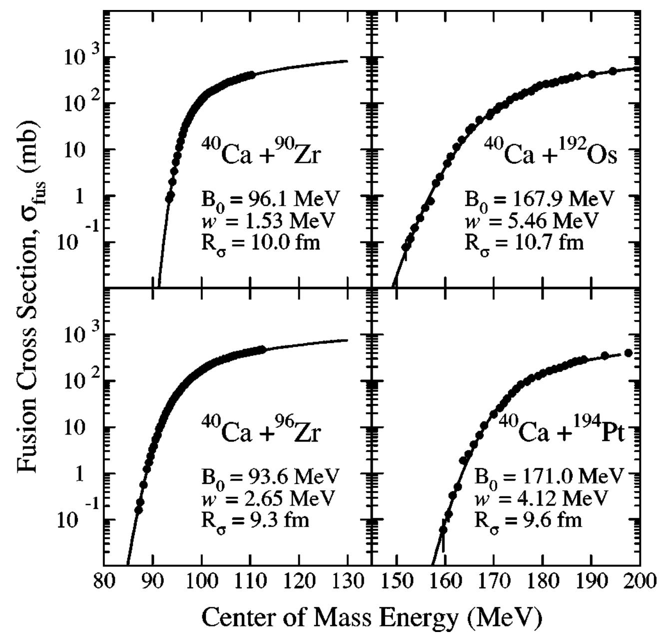

FIG. 6. Fusion excitation functions measured for the ^{40}Ca $+^{90,96}$Zr [12], ^{40}Ca$+^{192}$Os, and ^{40}Ca$+^{194}$Pt [11] reactions (full circles) compared with predictions (solid lines) of the "diffused-barrier formula," Eq. (6), for values of B_0, w and R_σ obtained with the least-square method.

tions *directly* determined by the double differentiation of $E\sigma$. It is clearly seen that the overall features of the barrier distributions, i.e., the position of the maximum and the width of the distribution, are perfectly reproduced by the Gaussian curves determined with Eq. (6). Therefore, as long as only those overall characteristics of the barrier distributions are concerned, one can use our easy method of analysis of experimental data with Eq. (6). An advantage of this simple method is that information on the parameters of the barrier distribution can be obtained in this way even from less precise experimental data—not accurate enough for reliable determination of the second derivative $d^2(E\sigma)/dE^2$.

It is very fortunate that the mean barrier B_0 and the width w are practically independent of the third parameter, the radius R_σ that, as it is seen from Eq. (6), does not influence shape of the excitation function and only scales the absolute value of the cross section. Thus, the barrier distribution parameters B_0 and w are precisely determined in the rapidly rising part of the fusion excitation function in the sub-barrier region, while a value of the third parameter R_σ depends on *absolute* normalization of the measured cross sections. In most of experiments the absolute values of the cross section are known not better than within ±20%. Consequently, the parameter R_σ can be determined with an accuracy of about ±10%, but—as mentioned above—this large uncertainty in R_σ does not influence the accuracy of determination of B_0 and w.

In Figs. 4–6 we show fusion excitation functions precisely measured [8–12,14,19] at near-barrier energies for 12 reactions sampled from the collection of systems studied so far experimentally. For each reaction, the diffused-barrier formula, Eq. (6), was fitted to experimental points, and the parameters B_0, w, and R_σ were determined by the least-square method. It is seen from Figs. 4–6 that for all systems, the measured fusion excitation functions can be very accurately reproduced with formula (6) in the entire range of energies, including the most critical sub-barrier region. As discussed above, the radius parameter R_σ includes uncertainties in the absolute normalization of the cross sections, but this fact does not influence precision in determination of the barrier distribution parameters B_0 and w, which are uncoupled from R_σ.

In the present work we analyzed more experimental data than presented in Figs. 4–6. All the studied reactions are listed in Table I. For the analysis we selected experimental data [3–19] for 48 medium and moderately heavy nuclear systems, for which we can presume that the fusion cross section is nearly identical with the cross section for overcoming the potential-energy barrier. Complete list of the deduced values of the parameters B_0, w, and R_σ is given in Table I.

V. NUCLEUS-NUCLEUS POTENTIAL DEDUCED FROM B_0 VALUES

Precise information on the mean values of the fusion barrier B_0 for a large number of reactions listed in Table I can be used for determination of an effective nucleus-nucleus potential characterizing interaction of dinuclear systems in peripheral configurations. We will show that so determined nucleus-nucleus potential can be used for reliable predictions of the fusion barriers for not yet studied systems.

A. Nuclear potential

We assume that the nuclear part of the nucleus-nucleus potential has the Woods-Saxon shape,

TABLE I. Values of the mean barrier height B_0, width of the barrier height distribution w, and effective radius R_σ, deduced from the analysis of fusion excitation functions for 48 reactions, using the "diffused-barrier formula," Eq. (6). The reactions are listed in order of the increasing value of the parameter $z=Z_1Z_2/(A_1^{1/3}+A_2^{1/3})$. Theoretical values of B_0 and w are also shown (see text).

Reaction	z	Ref.	B_0 (MeV)	w (MeV)	R_σ (fm)	B_0 (theor) (MeV)	w (theor) (MeV)
^{48}Ca+^{48}Ca	55.03	[19]	51.2	1.11	11.2	50.06	1.25
^{30}Si+^{64}Ni	55.16	[7]	51.4	1.38	9.6	50.85	1.39
^{30}Si+^{62}Ni	55.48	[7]	52.1	1.55	9.7	51.19	1.42
^{28}Si+^{64}Ni	55.71	[7]	50.4	1.12	7.6	51.29	1.43
^{28}Si+^{62}Ni	56.04	[7]	51.3	1.20	7.7	51.67	1.46
^{30}Si+^{58}Ni	56.18	[7]	52.8	1.59	8.8	51.84	1.36
^{40}Ca+^{48}Ca	56.70	[19]	51.8	1.78	11.5	51.97	1.31
^{28}Si+^{58}Ni	56.75	[7]	52.9	1.32	8.1	52.43	1.41
^{40}Ca+^{44}Ca	57.55	[5]	51.8	1.59	7.9	52.79	1.35
^{40}Ca+^{40}Ca	58.48	[5]	53.6	1.60	9.5	53.79	1.40
^{36}S+^{64}Ni	61.35	[7]	56.8	1.17	8.5	56.89	1.46
^{34}S+^{64}Ni	61.88	[7]	56.9	1.25	8.5	57.35	1.48
^{40}Ca+^{50}Ti	61.94	[13]	57.3	1.72	9.4	57.15	1.40
^{40}Ca+^{48}Ti	62.37	[13]	57.1	1.50	9.4	57.57	1.42
^{32}S+^{64}Ni	62.44	[7]	57.3	1.57	8.1	57.77	1.52
^{36}S+^{58}Ni	62.46	[7]	58.4	1.53	7.7	57.91	1.42
^{40}Ca+^{46}Ti	62.83	[13]	57.3	1.45	9.4	58.20	1.44
^{16}O+^{154}Sm	62.94	[10]	58.4	2.25	9.6	59.49	2.38
^{34}S+^{58}Ni	63.01	[7]	58.5	1.25	7.6	58.49	1.45
^{17}O+^{144}Sm	63.49	[10]	60.6	2.06	10.8	60.14	1.59
^{16}O+^{148}Sm	63.51	[10]	59.4	1.98	10.2	60.10	1.93
^{32}S+^{58}Ni	63.59	[7]	59.6	1.35	8.3	59.07	1.48
^{16}O+^{144}Sm	63.91	[10]	60.5	1.45	10.3	60.61	1.64
^{16}O+^{186}W	71.95	[10]	68.3	2.29	10.6	68.67	2.43
^{16}O+^{208}Pb	77.68	[14]	73.6	1.57	10.5	75.40	1.72
^{36}S+^{96}Zr	81.21	[16]	74.9	1.34	11.0	76.33	2.31
^{36}S+^{90}Zr	82.23	[16]	77.0	1.24	10.8	77.47	1.60
^{36}S+^{110}Pd	90.94	[9]	85.5	1.91	8.2	86.34	2.61
^{32}S+^{110}Pd	92.39	[9]	86.3	2.63	8.0	87.27	2.65
^{64}Ni+^{64}Ni	98.00	[4]	92.7	1.58	7.8	92.85	2.07
^{58}Ni+^{64}Ni	99.61	[4]	94.6	2.18	6.5	94.42	1.97
^{40}Ca+^{96}Zr	100.01	[12]	93.6	2.65	9.3	94.52	2.79
^{58}Ni+^{60}Ni	100.70	[8]	96.6	1.93	7.5	95.81	1.87
^{40}Ca+^{90}Zr	101.25	[12]	96.1	1.53	10.0	96.31	1.90
^{58}Ni+^{58}Ni	101.27	[3]	95.8	1.18	6.0	96.49	1.88
^{40}Ar+^{122}Sn	107.40	[6]	103.6	2.58	9.8	103.24	1.94
^{40}Ar+^{116}Sn	108.47	[6]	103.3	2.23	8.7	104.25	1.98
^{40}Ar+^{112}Sn	109.22	[6]	104.0	2.26	8.9	105.01	2.01
^{64}Ni+^{74}Ge	109.29	[4]	103.2	1.97	6.5	104.50	3.09
^{58}Ni+^{74}Ge	111.04	[4]	106.8	2.96	7.0	105.96	3.05
^{40}Ca+^{124}Sn	118.95	[15]	113.4	2.75	9.6	114.19	2.13
^{28}Si+^{198}Pt	123.18	[17]	120.9	3.41	9.8	120.48	2.94
^{34}S+^{168}Er	124.24	[18]	121.5	4.21	10.3	121.21	4.55
^{40}Ar+^{154}Sm	127.11	[6]	121.0	3.40	7.3	123.80	4.27
^{40}Ar+^{148}Sm	128.14	[6]	124.7	3.15	8.5	125.01	3.15
^{40}Ar+^{144}Sm	128.85	[6]	124.4	2.19	8.3	125.93	2.31

TABLE I. (*Continued.*)

Reaction	z	Ref.	B_0 (MeV)	w (MeV)	R_σ (fm)	B_0 (theor) (MeV)	w (theor) (MeV)
$^{40}Ca+^{192}Os$	165.42	[11]	167.9	5.46	10.7	164.80	4.18
$^{40}Ca+^{194}Pt$	169.40	[11]	171.0	4.12	9.6	169.60	4.20

$$V_n(r) = \frac{-V_0}{1+\exp\,[(r-R_1-R_2)/a]}, \tag{8}$$

where R_1 and R_2 are the radii of the two nuclei, r is their relative distance (well defined only for $r > R_1+R_2$), and a is the diffuseness parameter. For simplicity, we scale the radii R_i using a single parameter $r_0 = R_i/A_i^{1/3}$. Equation (8) represents a smooth and realistic interpolation of the nuclear potential energy of a given dinuclear system between the initial configuration of two noninteracting nuclei (of the ground-state masses M_1 and M_2 at the infinite distance $r=\infty$) and the final configuration at $r=0$ corresponding to the fused system, i.e., the compound nucleus of the ground-state mass M_{cn}. In order to single out nuclear interaction, we need to subtract from the total energy of the two initial nuclei and the final compound nucleus their intrinsic Coulomb energies, C_1, C_2 and C_{cn}, respectively. Thus the depth of the nuclear part of the potential for the fusion process is

$$V_0' = (M_1+M_2-M_{cn})c^2 + C_{cn} - C_1 - C_2, \tag{9}$$

where

$$\begin{aligned} C_{cn} - C_1 - C_2 &= C_0 \\ &= 0.7054\left[\frac{(Z_1+Z_2)^2}{(A_1+A_2)^{1/3}} - \frac{Z_1^2}{A_1^{1/3}} - \frac{Z_2^2}{A_2^{1/3}}\right]\text{MeV}. \end{aligned} \tag{10}$$

Here, the Coulomb energy constant is taken from the standard liquid-drop-model fit to nuclear masses [22]. To calculate V_0 in Eq. (8) we correct the depth V_0' of Eq. (9) by subtracting from the ground-state energy of the compound nucleus the shell correction energy S_{cn} because it produces only a very *local* dip (near the equilibrium shape) in the flat landscape of the nuclear potential energy described by the inner part of the Woods-Saxon potential. Thus

$$V_0 = V_0' + S_{cn} = Q_{fus} + C_0 + S_{cn}, \tag{11}$$

where by Q_{fus} we denote the ground-state Q value for fusion, $Q_{fus} = (M_1+M_2-M_{cn})c^2$, and C_0 is given by Eq. (10). The inclusion of the shell correction energy in Eq. (11) is almost insignificant for the potential in the peripheral region. The only role of S_{cn} in Eq. (11) is to consistently describe the total *macroscopic* potential energy for mononuclear shapes at small values of r, as it is seen by the fusing system. In our calculations we used S_{cn} values from the mass tables of Ref. [23].

B. Nuclear plus Coulomb potential

For typical applications, such as determination of the fusion barrier, it is sufficient to consider the nucleus-nucleus potential only in the outer region $r > R_1+R_2$. For that region, we use the point-charge approximation for the Coulomb potential, sufficiently accurate in the whole outer region of relative distances:

$$V(r) = V_n(r) + \frac{Z_1Z_2e^2}{r} \quad (\text{for outer distances } r). \tag{12}$$

For the inner range of distances r we put just the constant, asymptotic value of the potential energy of the completely fused system $(r=0)$:

$$V(r) = C_0 - V_0 = -Q_{fus} - S_{cn} \quad (\text{for inner distances } r). \tag{13}$$

Equation (12) is replaced by Eq. (13) below the crossing of these two expressions at the smallest distance.

C. Parameters of the empirical fusion potential

Equation (12) gives the total potential energy of a given nucleus-nucleus system as a function of the distance variable r, thus determining the height of the fusion barrier. There are only two free parameters in the expressions for the nucleus-nucleus potential: the radius parameter r_0 and the diffuseness of the nuclear potential a. We have determined these two parameters by fitting the barrier heights calculated with Eq. (12) to the set of the B_0 values obtained in our analysis described in the preceding section and listed in Table I. By applying the least-square method we have determined the best fitting parameters of the nuclear potential, Eqs. (8) and (11), as $r_0 = 1.18$ fm and $a = 0.675$ fm. These values correspond to location of the absolute minimum of χ^2, see Fig. 7. Viewing contours of a constant value of χ^2, we can see that there is a limited uncertainty in determination of r_0 and a along a narrow valley given by the relation

$$a = 2.9r_0^2 - 9.8r_0 + 8.2\ \text{fm}. \tag{14}$$

It is important to note that separate analysis of light, medium, and heavy systems shows that best combinations of the parameters a and r_0 for these separated groups of reactions are always located along the locus of Eq. (14), but there is a clear systematic trend: for heavier systems the optimum combination of a and r_0 moves along the locus (14) towards smaller r_0 and larger a values. Therefore we propose to limit validity of the global-fit parameters $r_0 = 1.18$ fm, a

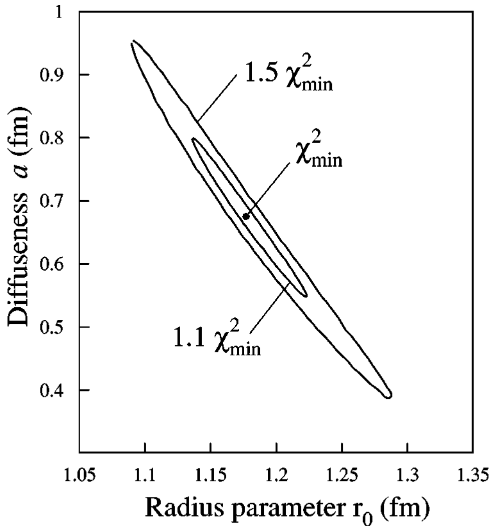

FIG. 7. Contours of constant value of χ^2 in the procedure of fitting the complete set of experimental fusion barriers B_0(exp) with those calculated with the Woods-Saxon nuclear potential, Eqs. (8) and (11). The best fit (χ^2_{min}) was found for $r_0=1.18$ fm and $a=0.675$ fm. The contours correspond to χ^2 increased by 10% and 50% relative to χ^2_{min}, respectively.

$=0.675$ fm only to medium systems characterized by a limited range of the Coulomb barrier parameter $z=Z_1Z_2/(A_1^{1/3}+A_2^{1/3})$:

$$r_0 = 1.18 \text{ fm}, \quad a = 0.675 \text{ fm} \quad \text{for} \quad 70 \leqslant z \leqslant 130, \tag{15}$$

and to use different values of the parameters for light and heavy systems:

$$r_0 = 1.25 \text{ fm}, \quad a = 0.481 \text{ fm} \quad \text{for} \quad z < 70, \tag{16}$$

and

$$r_0 = 1.11 \text{ fm}, \quad a = 0.895 \text{ fm} \quad \text{for} \quad z > 130. \tag{17}$$

The latter combination of parameters, Eq. (17), is suitable for predicting "sticking" or overcoming-the-barrier cross sections in reactions used to produce superheavy nuclei.

The barriers calculated for the nuclear potential with a and r_0 given by Eqs. (15)–(17) are listed in Table I. The root-mean-square deviation from experimental B_0 values is $(\delta B_0)_{rms}=1.05$ MeV, while for a fit with the fixed combination of the parameters $r_0=1.18$ fm and $a=0.675$ fm for all systems is $(\delta B_0)_{rms}=1.23$ MeV.

In Fig. 8 we compare experimental B_0 values with barrier heights calculated with three different nuclear potentials: (a) the potential determined in this work, (b) the Akyüz-Winther potential [24] frequently used in the coupled-channel calculations, and (c) the proximity potential recently modified by Myers and Świątecki [25]. It is seen that predictions based on our "empirical potential" agree quite well with experimental values of the mean barrier height B_0 showing no systematic deviations. On the contrary, calculations with the Akyüz-Winther potential systematically overestimate the fusion barriers. The difference $B_{theor}-B_0$ increases with increasing the Coulomb barrier parameter $z=Z_1Z_2/(A_1^{1/3}+A_2^{1/3})$, and the largest discrepancy of about 5 MeV is observed for the heaviest studied systems. Still larger discrepancies, up to 8 MeV, are observed for fusion barriers calculated with the proximity potential [see Fig. 8(c)].

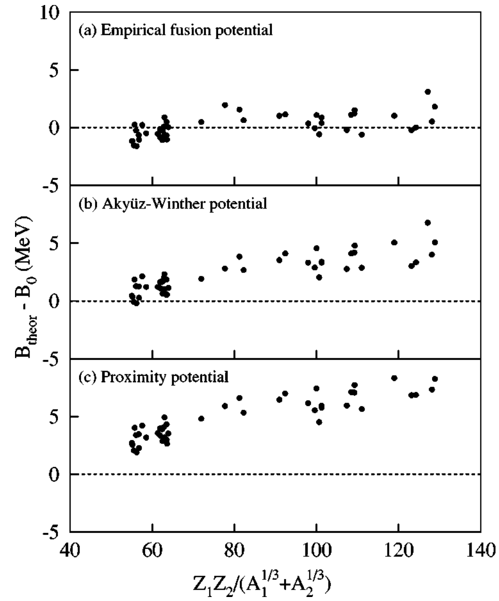

FIG. 8. Comparison of experimental barrier heights B_0 with theoretical predictions for the Akyüz-Winther potential [24], proximity potential [25], and the "empirical potential," Eqs. (8) and (11), with parameters r_0 and a given by Eq. (15).

VI. THEORETICAL ESTIMATES OF THE WIDTH *w*

As it is seen from Table I, the widths w of the barrier distributions deduced from experimental data are very diversified and show a strong dependence on individual properties of both fusing nuclei. In the following we derive a simple expression for w that accounts for the quantum effect of sub-barrier tunneling, as well as for static quadrupole deformations and collective surface vibrations of the colliding nuclei.

A. Sub-barrier tunneling

The effect of sub-barrier tunneling is accounted for in the analytic formula derived by Wong [26]:

$$\sigma_{fus}^{Wong} = \frac{\hbar\omega R^2}{2E}\ln\left[1 + \exp\frac{2\pi(E-B)}{\hbar\omega}\right]. \tag{18}$$

This formula predicts the cross section for overcoming the potential energy barrier B at an energy E, assuming the parabolic shape of the barrier with the curvature $\hbar\omega$ determined by second derivative of the potential at the top of the barrier:

$$\hbar\omega = \sqrt{\frac{\hbar^2}{\mu}\frac{d^2V(r)}{dr^2}}\Bigg|_{r=R}, \tag{19}$$

where μ is the reduced mass of the fusing system.

Rowley, Satchler, and Stelson [1] used the Wong formula (18) to determine the effective width of the barrier distribution associated with the sub-barrier tunneling:

$$\frac{1}{\pi R^2}\frac{d^2(E\sigma_{fus}^{Wong})}{dE^2} = G(x) = \frac{2\pi}{\hbar\omega}\frac{e^x}{(1+e^x)^2}, \tag{20}$$

where $x = 2\pi(E-B)/(\hbar\omega)$. Thus the width of the function $G(x)$ represents the width caused by the tunneling effect. [In the absence of tunneling, $G(x)$ would be just the δ function.] One can readily check that the root-mean-square width of the distribution $e^x/(1+e^x)^2$ is $\pi/\sqrt{3}$ and hence the width caused by the tunneling effect is

$$w_{tunnel} = \frac{\hbar\omega}{2\sqrt{3}}. \tag{21}$$

By calculating $\hbar\omega$ in Eq. (19) assuming purely exponential dependence of the nuclear potential [27], we obtain

$$(w_{tunnel})^2 = \frac{Z_1 Z_2 e^2 \hbar^2}{12\mu R^2}\left(\frac{1}{a} - \frac{2}{R}\right), \tag{22}$$

where a is a parameter in the exponent describing the nuclear potential $V_n(r) \sim \exp(-r/a)$.

B. Static deformations

Following Ref. [28], we propose a simple expression to estimate the contribution of nuclear static deformations to the magnitude of the width w. Assuming all possible orientations of a nucleus i with a static deformation $\beta_2(i)$, one obtains the variation of the effective radius $R(i)$ with the standard deviation,

$$\Delta R_i = \frac{\beta_2(i)}{\sqrt{4\pi}} R_i. \tag{23}$$

The distribution of the resulting surface-surface distance (for a fixed distance between centers of mass of the two nuclei) leads to a distribution of the barrier height with the standard deviation,

$$w_{stat}(i) = \Delta R_i \frac{\partial V_{\lambda=2}(i)}{\partial r} = \frac{\beta_2(i)}{\sqrt{4\pi}} R_i \left[-\frac{dV_n}{dr} + \frac{3Z_1Z_2e^2}{5}\frac{R_i}{r^3}\right]_{r=R}, \tag{24}$$

where the expression for the derivative $\partial V_{\lambda=2}(i)/\partial r$ for quadrupole deformations follows Refs. [28,29]. Since at distances in vicinity of the barrier

$$\left.\frac{dV_n}{dr}\right|_{r=R} \approx \frac{Z_1 Z_2 e^2}{R^2}, \tag{25}$$

we obtain

$$w_{stat}(i) = \frac{Z_1 Z_2 e^2}{R}\frac{\beta_2(i)}{\sqrt{4\pi}}\left(\frac{3}{5}\frac{R_i^2}{R^2} - \frac{R_i}{R}\right). \tag{26}$$

As the *static* deformations we have taken *theoretical* values of β_2 from Ref. [23], however for all light nuclei of $A \leqslant 30$ we have put $\beta_2 = 0$.

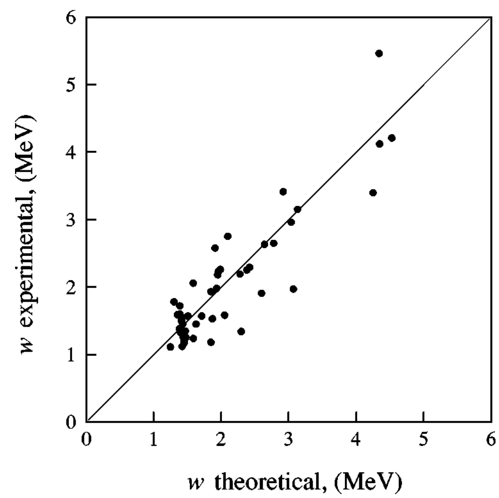

FIG. 9. Comparison of experimental values of the width w of the fusion barrier distributions, deduced for 48 reactions (fifth column in Table I) with those calculated with Eq. (27).

C. Calculations of the total width

In addition to the rotational smearing of the barrier height, Eqs. (26), we assume also a possible contribution from vibrational degrees of freedom. However, we treat this contribution in an extremely simplified way assuming the same relative amplitude of the vibration for all nuclei. [We put a constant value of $\beta_2^{vibr}(i)$ into respective expressions for $w_{vibr}(i)$, analog to Eq. (26).] Thus, in fact, β_2^{vibr} is an adjusting parameter of the model.

Summing up quadratically all components, the total width w is given by the expression

$$w = \sqrt{w_{tunnel}^2 + w_{stat}^2(1) + w_{stat}^2(2) + w_{vibr}^2(1) + w_{vibr}^2(2)}, \tag{27}$$

which contains only one free parameter β_2^{vibr}. From best χ^2 fit of expression (27) to our set of empirical values of w (see Table I), we obtained $\beta_2^{vibr} = 0.12$. Values of the width w calculated with Eq. (27) are shown in the last column of Table I, and their correlation with experimental values is shown in Fig. 9. The accuracy of predictions of the formula (27) is $\Delta w/w \approx \pm 20\%$.

VII. PREDICTIONS OF FUSION CROSS SECTIONS AND SUMMARY

Results of our analysis presented in previous sections open the way to predict fusion excitation functions for not yet studied nuclear systems. (Strictly speaking, we can predict only the "overcoming-the-barrier" cross sections which—as discussed in Sec. V—are not identical with fusion cross sections in the case of very heavy systems.) To calculate the overcoming-the-barrier cross section for a given projectile-target combination one can use Eq. (6) applying theoretical values of the parameters B_0 and w. The barrier height B_0 can be readily calculated with the nuclear potential, Eqs. (8) and (11), using values of r_0 and a as determined empirically, Eqs. (15)–(17). The width w can be predicted with a reasonable accuracy by using Eq. (27). We propose to take the third parameter used in formula (6) R_σ as

$$R_\sigma = r_\sigma (A_1^{1/3} + A_2^{1/3}) \text{ fm}, \tag{28}$$

where the coefficient $r_\sigma = 1.16$ fm is the average value of r_σ for the whole set of systems listed in Table I. As discussed in Sec. IV, systematic errors resulting from uncertainties of absolute normalization of the cross sections cause that the values of r_σ are quite widely scattered ($r_\sigma = 1.16 \pm 0.19$ fm). However, the average value obtained from results of many independent experiments is expected to be determined more accurately.

In summary, we have studied an ample set of precisely measured fusion excitation functions with the aim to learn about conditions of overcoming the potential energy barrier in nucleus-nucleus collisions. We attempted to obtain systematic information on the essential characteristics of the potential interaction between two nuclei, the mean barrier height B_0 and width w of its distribution. For the analysis of experimental data we used the simple diffused-barrier formula, Eq. (6), derived under assumption of the Gaussian shape of the barrier distribution. By using Eq. (6) for typical excitation functions, measured with high precision required to determine the Rowley's derivative $d^2(E\sigma)/dE^2$, the mean values of the barrier B_0 have been deduced with an accuracy significantly better than ± 1 MeV.

We have used the obtained set of precisely determined B_0 values to establish an effective nucleus-nucleus potential in order to use it then for predicting the barrier heights and fusion (or capture) cross sections for not yet studied systems. It is assumed that the nuclear part of the proposed potential, Eqs. (8) and (11), has Woods-Saxon shape, and aims for small relative distances at the energy of the fused system. The only two free parameters a and r_0, Eqs. (15)–(17), have been determined from the best fit to B_0 values for 48 different nuclear systems. The mean barrier heights calculated with this potential are reproduced with an accuracy of about 1 MeV. We demonstrated that other frequently used potentials, the proximity potential [25] and the Akyüz-Winther potential [24], considerably overpredict the barrier heights, especially, for heavy systems.

We propose a simple method of theoretical estimation of the width of the barrier distribution. The proposed formula, Eq. (27), accounts for the quantum effect of sub-barrier tunneling, static quadrupole deformations, and collective surface vibrations of the colliding nuclei.

Theoretical knowledge of both, the mean barrier B_0 and width w enables us to use the diffused-barrier formula, Eq. (6), and to predict cross sections for overcoming the barrier in collisions of very heavy systems used to produce superheavy nuclei. In such a way we are able to predict the energy dependence of the cross section for capture or sticking in these reactions, one of three basic ingredients in the sticking-diffusion-survival model [21] for calculating the production cross sections of superheavy nuclei.

ACKNOWLEDGMENTS

We would like to thank W. J. Świątecki for many inspiring discussions and his constant interest in this study. We also thank Ch. Droste for discussions and J. Błocki for providing us with a computer code for calculating the proximity potential.

[1] N. Rowley, G. R. Satchler, and P. H. Stelson, Phys. Lett. B **245**, 25 (1991).

[2] M. Dasgupta, D. J. Hinde, N. Rowley, and A. M. Stefanini, Annu. Rev. Nucl. Part. Sci. **48**, 401 (1998).

[3] M. Beckerman, M. Salomaa, A. Sperduto, H. Enge, J. Ball, A. DiRienzo, S. Gazes, Yan Chen, J. D. Molitoris, and Mao Naifeng, Phys. Rev. Lett. **45**, 1472 (1980).

[4] M. Beckerman, M. Salomaa, A. Sperduto, J. D. Molitoris, and A. DiRienzo, Phys. Rev. C **25**, 837 (1982).

[5] H. A. Aljuwair, R. J. Ledoux, M. Beckerman, S. B. Gazes, J. Wiggins, E. R. Cosman, R. R. Betts, S. Saini, and Ole Hansen, Phys. Rev. C **30**, 1223 (1984).

[6] W. Reisdorf, F. P. Hessberger, K. D. Hildebrand, S. Hofmann, G. Münzenberg, K.-H. Schmidt, J. H. R. Schneider, W. F. W. Schneider, K. Sümmerer, G. Wirth, J. V. Kratz, and K. Schlitt, Nucl. Phys. **A438**, 212 (1985).

[7] A. M. Stefanini, G. Fortuna, R. Pengo, W. Meczynski, G. Montagnoli, L. Corradi, A. Tivelli, S. Beghini, C. Signorini, S. Lunardi, M. Morando, and F. Soramel, Nucl. Phys. **A456**, 509 (1986).

[8] A. M. Stefanini, D. Ackermann, L. Corradi, D. R. Napoli, C. Petrache, P. Spolaore, P. Bednarczyk, H. Q. Zhang, S. Beghini, G. Montagnoli, L. Mueller, F. Scarlassara, G. F. Segato, F. Soramel, and N. Rowley, Phys. Rev. Lett. **74**, 864 (1995).

[9] A. M. Stefanini, D. Ackermann, L. Corradi, J. H. He, G. Montagnoli, S. Beghini, F. Scarlassara, and G. F. Segato, Phys. Rev. C **52**, R1727 (1995).

[10] J. R. Leigh, M. Dasgupta, D. J. Hinde, J. C. Mein, C. R. Morton, R. C. Lemmon, J. P. Lestone, J. O. Newton, H. Timmers, J. X. Wei, and N. Rowley, Phys. Rev. C **52**, 3151 (1995).

[11] J. D. Bierman, P. Chan, J. F. Liang, M. P. Kelly, A. A. Sonzogni, and R. Vandenbosch, Phys. Rev. C **54**, 3068 (1996).

[12] H. Timmers, D. Ackermann, S. Beghini, L. Corradi, J. H. He, G. Montagnoli, F. Scarlassara, A. M. Stefanini, and N. Rowley, Nucl. Phys. **A633**, 421 (1998).

[13] A. A. Sonzogni, J. D. Bierman, M. P. Kelly, J. P. Lestone, J. F. Liang, and R. Vandenbosch, Phys. Rev. C **57**, 722 (1998).

[14] C. R. Morton, A. C. Berriman, M. Dasgupta, D. J. Hinde, J. O. Newton, K. Hagino, and I. J. Thompson, Phys. Rev. C **60**, 044608 (1999).

[15] F. Scarlassara, S. Beghini, G. Montagnoli, G. F. Segato, D. Ackermann, L. Corradi, C. J. Lin, A. M. Stefanini, and L. F. Zheng, Nucl. Phys. **A672**, 99 (2000).

[16] A. M. Stefanini, L. Corradi, A. M. Vinodkumar, Yang Feng, F. Scarlassara, G. Montagnoli, S. Beghini, and M. Bisogno, Phys. Rev. C **62**, 014601 (2000).
[17] K. Nishio, H. Ikezoe, S. Mitsuoka, and J. Lu, Phys. Rev. C **62**, 014602 (2000).
[18] C. R. Morton, A. C. Berriman, R. D. Butt, M. Dasgupta, A. Godley, D. J. Hinde, and J. O. Newton, Phys. Rev. C **62**, 024607 (2000).
[19] M. Trotta, A. M. Stefanini, L. Corradi, A. Gadea, F. Scarlassara, S. Beghini, and G. Montagnoli, Phys. Rev. C **65**, 011601(R) (2001).
[20] K. Siwek-Wilczyńska, I. Skwira, and J. Wilczyński, Acta Phys. Pol. B **34**, 1867 (2003).
[21] W. J. Świątecki, K. Siwek-Wilczyńska, and J. Wilczyński, Acta Phys. Pol. B **34**, 2049 (2003).
[22] W. D. Myers and W. J. Swiatecki, Ark. Fys. **36**, 343 (1967).
[23] P. Möller, J. R. Nix, W. D. Myers, and W. J. Świątecki, At. Data Nucl. Data Tables **59**, 185 (1995).
[24] R. Ö. Akyüz and A. Winther, in *Nuclear Structure and Heavy-Ion Collisions*, Proceedings of the International School of Physics "Enrico Fermi," Course LXXVII, edited by R. A. Broglia, R. A. Ricci, and C. H. Dasso (North Holland, Amsterdam, 1981), p. 492; M. Dasgupta, A. Navin, Y. K. Agarwal, C. V. K. Baba, H. C. Jain, M. L. Jhingan, and A. Roy, Nucl. Phys. **A539**, 351 (1992).
[25] W. D. Myers and W. J. Świątecki, Phys. Rev. C **62**, 044610 (2000).
[26] C. Y. Wong, Phys. Rev. Lett. **48**, 766 (1973).
[27] N. Poffé, N. Rowley, and R. Lindsay, Nucl. Phys. **A410**, 498 (1983).
[28] H. Esbensen, Nucl. Phys. **A352**, 147 (1981).
[29] C. H. Dasso and S. Landowne, Comput. Phys. Commun. **54**, 187 (1987).